
Light
Scattering
Reviews 9
Alexander A. Kokhanovsky
Editor
Springer
PRAXIS

Light Scattering Reviews 9

Light Scattering and Radiative Transfer

Alexander A. Kokhanovsky (Editor)

Light Scattering Reviews 9

Light Scattering and Radiative Transfer

Springer

Published in association with
Praxis Publishing
Chichester, UK

PRAXIS

Editor
Dr. Alexander A. Kokhanovsky
Institute of Environmental Physics
University of Bremen
Bremen
Germany

SPRINGER–PRAXIS BOOKS IN ENVIRONMENTAL SCIENCES (LIGHT SCATTERING SUB-SERIES)
EDITORIAL ADVISORY BOARD MEMBER: Dr. Alexander A. Kokhanovsky, Ph.D., Institute of Environmental Physics, University of Bremen, Bremen, Germany

ISBN 978-3-642-37984-0 ISBN 978-3-642-37985-7 (eBook)
DOI 10.1007/978-3-642-37985-7
Springer Heidelberg New York Dordrecht London

Library of Congress Control Number: 2014950797

Cover design: Jim Wilkie
Project copy editor: Christine Cressy
Author-generated LaTex, processed by EDV-Beratung Herweg, Germany

Printed on acid-free paper

Springer is a part of Springer Science+Business Media (www.springer.com)

Contents

Part III Polarimetry

Part IV Radiative Forcing

List of Contributors

Ackerman, Andrew A.
Laboratory for Atmospheres
NASA Goddard Space Flight Center
Greenbelt, MD
USA
andrew.ackerman@nasa.gov

Adam, John A.
Department of Mathematics & Statistics
Old Dominion University
Norfolk, VA 23529
USA
jadam@odu.edu

Cairns, Brian
NASA Goddard Institute for Space Studies
New York, NY
USA
brian.cairns@nasa.gov

Cho, Hyoun-Myoung
Joint Center for Earth Systems Technology
Baltimore, MD
USA
hmcho@umbc.edu

Gritsevich, Maria
Finnish Geodetic Institute
Box 14
02431 Masala
Finland
maria.gritsevich@fgi.fi

Jethva, Hiren
NASA Goddard Space Flight Center
Greenbelt, MD
USA
hiren.jethva@nasa.gov

Kacenelenbogen, Meloe
BAER Institute
NASA Ames Research Center
Moffett Field, CA
USA
Meloe.Kacenelenbogen@nasa.gov

Kandler, Konrad
Institut für Angewandte Geowissenschaften-Fachgebiet Umweltmineralogie
Technische Universität Darmstadt
Schnittspahnstr. 9
D-64287 Darmstadt
Germany
kzk@gmx.de

Knobelspiesse, Kirk
NASA Ames Research Center
Moffett Field, CA
USA
kirk.d.knobelspiesse@nasa.gov

Lanconelli, Christian
Institute of Atmospheric Sciences and Climate (ISAC)
National Council of Research (CNR)
Area della Ricerca
Via Piero Gobetti 101
I-40129 Bologna
Italy
c.lanconelli@isac.cnr.it

Lupi, Angelo
Institute of Atmospheric Sciences and Climate (ISAC)
National Council of Research (CNR)
Area della Ricerca
Via Piero Gobetti 101
I-40129 Bologna
Italy
a.lupi@isac.cnr.it

Mazzola, Mauro
Institute of Atmospheric Sciences and Climate (ISAC)
National Council of Research (CNR)
Area della Ricerca
Via Piero Gobetti 101
I-40129 Bologna
Italy
m.mazzola@isac.cnr.it

Nousiainen, Timo
Finnish Meteorological Institute
Earth Observation
P.O. Box 503
FI-00101 Helsinki
Finland
timo.nousiainen@fmi.fi

Peltoniemi, Jouni I.
Finnish Geodetic Institute
Box 14
02431 Masala
Finland
jouni.peltoniemi@fgi.fi

Platnick, Steven
Laboratory for Atmospheres
NASA Goddard Space Flight Center
Greenbelt, MD
USA
steven.platnick@nasa.gov

Puttonen, Eetu
Finnish Geodetic Institute
Box 14
02431 Masala
Finland
eetu.puttonen@fgi.fi

Savenkov, Sergey N.
Department of Radiophysics
Taras Shevchenko National University
Vladimirskaya Str. 60
01033 Kiev
Ukraine
sns@univ.kiev.ua

Segal-Rosenheimer, Michal
BAER Institute
NASA Ames Research Center
Moffett Field, CA
USA
michal.segalrozenhaimer@nasa.gov

Sharma, Subodh K.
S. N. Bose National Centre for Basic Sciences
Block JD, Sector III
Salt Lake
Kolkata 700098
India
sharma@boson.bose.res.in

Tomasi, Claudio
Institute of Atmospheric Sciences and Climate (ISAC)
National Council of Research (CNR)
Area della Ricerca
Via Piero Gobetti 101
I-40129 Bologna
Italy
c.tomasi@isac.cnr.it

Torres, Omar
NASA Goddard Space Flight Center
Greenbelt, MD
USA
omar.torres@nasa.gov

Zhang, Zhibo
Physics Department
University of Maryland Baltimore County
Baltimore, MD
USA
zhibo.zhang@umbc.edu

Preface

This volume of *Light Scattering Reviews* is aimed at the presentation of recent advances in light scattering, polarimetry, remote sensing, and radiative forcing. It consists of eight chapters. The first chapter of the volume, prepared by *Timo Nousiainen* and *Konrad Kandler*, is devoted to the presentation of recent results related to light scattering by atmospheric mineral dust particles. These particles originate mostly from the arid and semi-arid regions, particularly from the deserts and their margins. The authors consider the physical properties of dust particles including chemical composition, their shape and structure, and also particle size distributions. Light-scattering measurements and modeling of light-scattering properties of atmospheric dust are reviewed at great depth. In particular, the impact of morphological details and anisotropy on scattering is discussed. *Subodh K. Sharma* gives a review of approximate analytical results for the scattering phase functions of various small particles. The closed-form solutions are of importance for the studies of radiative transfer processes in particulate matter and also for the aims of remote sensing, where the speed of calculations is of importance due to the large volume of data to be processed. *John A. Adam* gives a survey of literature related to the analytical solutions of the radial *TE* and *TM* mode electromagnetic equations for radially inhomogeneous media. The author gives also a brief discussion of the ray-theoretic approach to propagation in radially inhomogeneous media. The problems related to the satellite remote sensing of cloud droplet effective radii are discussed by *Zhibo Zhang et al. Kirk Knobelspiesse et al.* discuss the application of light scattering and radiative transfer to remote sensing of aerosol layers located above clouds. The next two chapters are devoted to the polarimetric studies of various objects. *Sergey Savenkov* discusses the principles of the Mueller matrix measurements, while *Jouni I. Peltoniemi et al.* present results of measurements of the intensity and polarization of light reflected from various vegetated surfaces. The results are of importance for the remote sensing of atmosphere and underlying surface using airborne and space-borne instrumentation. The concluding section, prepared by *Claudio Tomasi et al.*, is aimed at the discussion of the direct aerosol-induced radiative forcing from clear-sky field measurements performed during seven regional experiments.

Bremen, Germany
December, 2013

Alexander A.Kokhanovsky

Part I

Light Scattering

1 Light scattering by atmospheric mineral dust particles

Timo Nousiainen and Konrad Kandler

1.1 Introduction

When discussing atmospheric aerosol particles, mineral dust refers to suspended soil-constituting mineral particles that originate mainly from arid and semi-arid regions, particularly from deserts and their margins. These particles constitute one of the most prominent aerosol classes in Earth's atmosphere and exert a considerable impact on radiation in the atmosphere. In addition, mineral dust particles act as ice nuclei and under some conditions as condensation nuclei, thus also indirectly impacting radiation and contributing to the global water cycle. Furthermore, dust particles are the main source of iron for ocean surface waters outside continental margins. Mineral dust is therefore a highly important atmospheric constituent.

To quantify the radiative effect of mineral dust, to monitor their presence and abundance in the atmosphere with remote sensing methods, or to correct for their impact in other types of atmospheric remote sensing applications, dust particles' single-scattering properties are needed. These properties depend on the sizes, shapes, and compositions of the dust particles, as well as the wavelength of incident radiation. Computing the single-scattering properties accurately is a great challenge, in part due to the great complexity of the particles, and in part for the lack of suitable, exact light-scattering methods that could be applied to such targets.

This chapter aims at reviewing the current understanding of the dust particle properties, and critically assessing different modeling approaches adapted to model their single-scattering properties. To keep the chapter from getting overly extensive, we do not elaborate on the merits of different light-scattering codes or the underlying theories. On the other hand, we will shortly introduce light-scattering measurements, because of their central role in assessing the performance of the modeling approaches. Regarding measurements, we mainly consider those carried out in a laboratory, where the physical properties of the target particles can also be analyzed. Therefore, a vast amount of literature related to remote sensing of mineral dust has been left out. Also, we only focus on the single-scattering properties and do not consider how uncertainties in them translate into uncertainties in remote sensing or radiative forcing estimates. Finally, we only consider single-scattering properties related to elastic scattering.

A. Kokhanovsky (ed.), *Light Scattering Reviews 9*, Springer Praxis Books,
DOI 10.1007/978-3-642-37985-7_1

The chapter is organized as follows. The physical dust particle properties are reviewed in section 1.2, with separate subsections for shape, composition, structure (1.2.1), and size distributions (1.2.2). Section 1.3 shortly outlines controlled light-scattering measurements and their role in validation of the approaches used for dust particles' light-scattering modeling. Those appoaches are assessed in section 1.4, with separate subsections for the theoretical concepts and definitions (1.4.1), approaches based on simple (1.4.2) and complex (1.4.3) geometries, as well as pure modeling studies assessing the impact of different morphological details, namely surface roughness, internal inhomogeneity, and material anisotropy on scattering (1.4.4). The discussion, conclusions, and an outlook for the future are presented in section 1.5.

1.2 Physical properties of dust particles

To properly model the single-scattering properties of dust particles, it is important to understand the physical properties, namely the structure, shape, and composition of these particles. This section provides, in the first part, an introduction to the radiation-relevant compositional properties of mineral particles, including characteristic structure types and their influence on particle shape. The second part deals with particle size distributions and their evolution.

1.2.1 Composition, structure, and shape

The major constituents of mineral dust particles are different mineral species. A mineral is a naturally occurring solid substance with specific chemical composition and ordered atomic structure. For our purposes, mineral dust can be defined as atmospheric aerosol derived from minerals constituting the soil. As such, it may consist of any mineral species present in the soil, but excludes the organic compounds. It should be noted, however, that there exist other definitions – that is, i.e., some authors exclude soluble species like sulfates or nitrates, while others define mineral dust by analysis technique and location, such as the refractory, crystalline, or the insoluble fraction of the aerosol, collected downwind from a known mineral dust source. Here, we follow the definition of the soil-derived matter, but discuss also soluble material, undistinguished as to whether it comes from the original soil or from atmospheric processing. As the strongest dust sources are the warm deserts (e.g. Zender et al., 2003), mineral dust is referred to as desert dust by many authors.

The dust composition can be assessed by a number of methods, none of which provides the complete information on its own. Bulk samples – for example, filter samples – are commonly analyzed using X-ray fluorescence (XRF), proton-induced X-ray fluorescence (PIXE), X-ray diffraction (XRD), Fourier-transform infrared (FTIR), or Raman spectroscopy. From XRF and PIXE, elemental concentrations and their ratios are obtained, from which the composition in terms of mineral species has to be derived, making assumptions based on a known soil composition or common frequency of occurrence. XRD, in contrast, is able to detect crystal lattice characteristics and, thus, provides information on mineral species directly. However, it is not equally sensitive to all minerals (in particular, less to clay minerals),

and some mineral groups are difficult to distinguish. Also, it has a rather high detection limit (absolute as well as relative), and it can only detect (well-)crystallized species (e.g. no glassy or micro-crystalline materials). FTIR can also provide information on particular mineral species by identifying stretching vibrations in bonds but, like XRD, it suffers from ambiguity and sometimes lacks reference spectra. Raman spectroscopy can also be applied to assess the mineralogical composition (e.g. Stefaniak et al., 2006; Sobanska et al., 2012), but apparently has never been used extensively for atmospheric dust.

Samples, from which individual particles can be analyzed, are usually subject to electron-microscopic analysis, but are sometimes also analyzed by micro-XRF/PIXE or Raman microscopy. These methods are rather labor-intensive, so the data basis is small. From electron microscopy, usually also an XRF signal is obtained. It has larger uncertainties than bulk XRF but, on the other hand, provides high-resolution images from which characteristic morphology can be taken into account. If transmission electron microscopy is used, the electron diffraction pattern can be analyzed and information on the crystal structure extracted, so a true mineral species determination can be performed. Raman or FTIR microscopy yields a considerably lower image resolution than electron microscopy, but provides information on the bonding state, allowing conclusions on the mineral species to be drawn.

Based on the variability of the source soils, the composition of atmospheric dust may also vary considerably. The only components that have been reported at every location studied are quartz and phyllosilicates in general. Of the large phyllosilicates group, illite and/or kaolinite are most common, but also chlorite, muscovite, montmorillonite, biotite, palygorskite, smectites, and inter-stratified clay minerals are often reported (e.g., Formenti et al., 2011; Scheuvens et al., 2013; and references therein). Note that most of these mineral denominations still refer only to mineral groups, as the actual mineral species were not determined. In many cases, additional silicate minerals are reported: feldspars like albite, anorthite, and potassium feldspars, less frequently orthoclase, or other phyllosilicates like chrysotile. In varying abundance and depending on the source region, calcite, dolomite, and, more rarely, apatite are found. Also in its abundance depending on the source, the iron compounds hematite and goethite are reported, less frequently also ilmenite.

The most common soluble species accompanying the insoluble ones are sulfates, nitrates, and chlorides, which are not reported with a specific mineral denomination as they usually recrystallize in the atmosphere quickly and fractionally, depending on the environmental conditions. In addition to the above-mentioned major dust components, a multitude of rarer mineral species are reported in the literature, namely biological debris like diatomite; metal oxides like rutile, periclase, baddeleyite, or spinel; other iron-rich minerals like lepidocrocite or limonite; different carbonates such as aragonite or magnesite; more or less soluble sulfates like anhydrite, gypsum, thenardite, mirabilite, mascagnite, and glauberite; and silicates like chloritoid, leucite, forsterite, zircon, or enstatite (Glaccum and Prospero, 1980; Leinen et al., 1994; Merrill et al., 1994; Molinaroli, 1996; Caquineau et al., 2002; Shao et al., 2007; Jeong, 2008; Journet et al., 2008; Kandler et al., 2009; Shen et al., 2009; Kendler et al., 2011b; Wang et al., 2012).

With respect to its natural variability, it is not possible to calculate a representative average dust composition. Instead, there have been regionally resolved compilations of dust composition as a function of provenance (e.g. Formenti et al., 2011; Scheuvens et al., 2013) or modeled compositions derived from the more or less well-known soil compositions (e.g. Claquin et al., 1999; Nickovic et al., 2012). These compilations present some general trends for the dust composition, but the variability can be very high even on a small scale (see, e.g. data of Bristow et al. (2010) for the Bodélé depression, in which the calcium-to-iron ratio varies over the same range as for the whole Saharan Desert; Scheuvens et al., 2013). As an example for atmospheric measurement data, Fig. 1.1 illustrates the temporal variation of dust composition in Morocco and Cape Verde. While quartz, K-feldspars, and illite usually dominate the aerosol in Morocco, kaolinite and K-feldspars are the major components at Cape Verde, with additional marine contributions in halite and gypsum that are expectedly absent in Morocco. Besides the major difference in clay minerals, the feldspars of the plagioclase group are more common in Cape Verde. The temporal variability becomes obvious between dusty and cleaner periods as well as within single intense dust periods: in Morocco, the dominant compound switches between quartz, K-feldspars, and illite, but calcite is also a major component on certain days. A similar behavior is visible for plagioclases, K-feldspars, and kaolinite at Cape Verde.

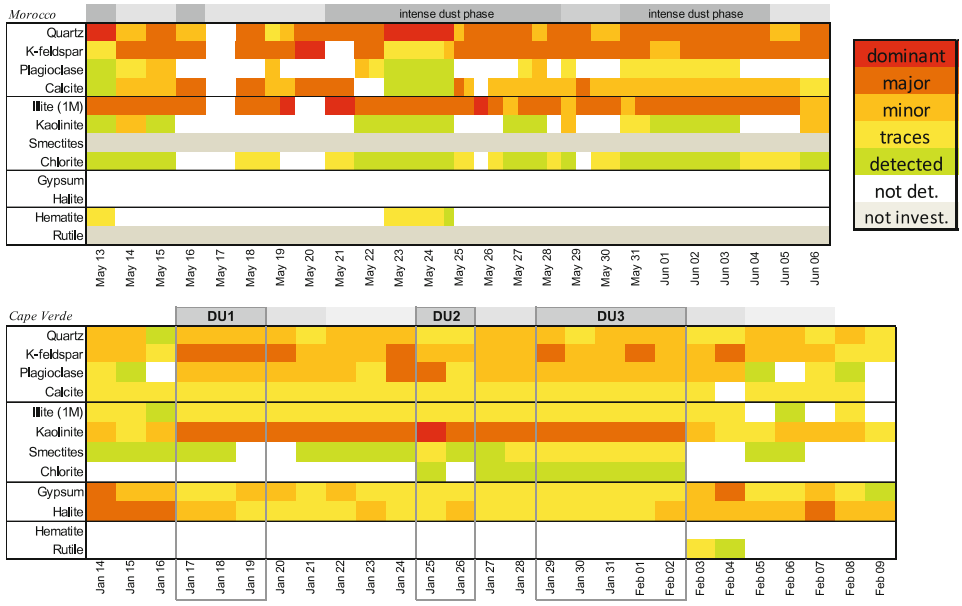

Fig. 1.1. Crystalline aerosol components observed in Morocco in 2006 and at Cape Verde in 2008, determined by X-ray diffraction of filter samples. Dust concentration of the several periods is shown as the graylevel on top with the most intense periods marked. For details about the locations, sampling and analysis, see Kandler et al. (2009, 2011b).

Beyond the variability in bulk composition, there is variation between single dust particles. Desert dust in particular is a mixture of single- and multi-mineral grains, where a single grain can consist of a nearly arbitrary combination of the minerals mentioned above. Figure 1.2 shows some discriminating elemental ratios for a few hundred individual dust particles from a single sample. We can observe some characteristic differences between Morocco and Cape Verde, such as lower calcium and higher iron contents as well as lower sodium and higher magnesium contents at Cape Verde than in Morocco. However, there is a very high inter-particle variation, which becomes especially obvious when we compare these data sets to the more uniform volcanic mineral particles, where most of the particles are supposed to have the same source (the melt) and the same age. Even there, a considerable variation in the calcium/iron ratio exists, but the variability in the other elemental ratios is much lower than for desert dust.

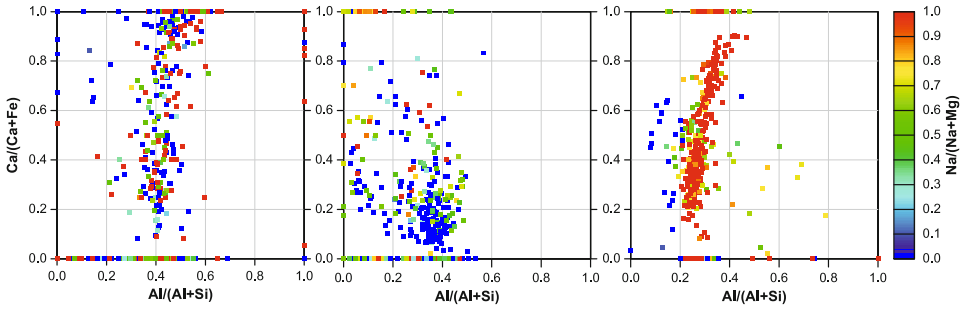

Fig. 1.2. Discriminating elemental atomic ratios for the mineral dust component of samples collected in Morocco (May 27, 2006; left panel), Cape Verde (Jan 29, 2008; center panel), and during the Eyjafjell volcano eruption (May 17, 2010; right panel); graphs drawn from data by Kandler et al. (2009, 2011a) and Schumann et al. (2011).

The composition of the mineral dust depends also on the particle size. Usually, it is assumed that the mechanically more stable minerals are less subject to abrasion and, thus, have larger particle sizes, while the less stable species subsequently exist in smaller particles. For example, Kandler et al. (2009) demonstrated that the largest particles with diameters $D > 50$ μm are dominated by quartz. Smaller ones consist of feldspars and clay minerals; the clay minerals usually dominate, and their fraction increases with decreasing particle size (Kandler et al., 2011a; Schütz and Rahn, 1982; Shi et al., 2005). If present, carbonates such as calcite or dolomite are usually found between $D = 1$ μm and 20 μm (Kandler et al., 2009).

Looking even closer, at the single-particle level, we observe that, for particles consisting of more than one mineral species, the compounds are anything but evenly distributed. In particular, clay minerals tend to form aggregates of several micrometers in diameter, in which grains of other substances are frequently embedded. Figure 1.3 (left) shows such a compact clay mineral aggregate. From the localized characteristic XRF, we find the presence of iron oxi(hydroxi)des and titanium oxides in small grains. Also, we can see that a quartz or feldspar grain must exist inside the particle, as there are no visible features corresponding with the

elevated silicon signal. Finally, phosphates and probably sulfates also exist within this aggregate.

Besides the occurrence of mixed particles, which are already formed prior to emission, mineral dust may be processed in the atmosphere by clouds (Sullivan et al., 2007a; Matsuki et al., 2010) or by non-cloud processes like condensation (Deboudt et al., 2010), heterogeneous reactions (Ullerstam et al., 2002; Usher et al., 2002), or sea-salt mixing (Zhang and Iwasaka, 2004). Depending on the composition of the individual particle, atmospheric processing might result in a coating or adhering of usually soluble substances (Kandler et al., 2011a; Deboudt et al., 2010; Li and Shao, 2009), or in a thoroughly processed particle (Krueger et al., 2003, 2004; Matsuki et al., 2005). While, in the latter case, nearly nothing is preserved from the original particle structure, an addition of a soluble substance might just cover some surface features of the original particle; also, it can be present in a single location or between insoluble mineral grains (e.g. Fig. 1.3 (right panel) and Fig. 1.4).

Subsequently, in an atmospheric mineral dust sample, we expect to find a mixture of different particle structures, depending on the parent soil and the atmospheric history. The structure types can be described as 'mono-grain', 'main grain with minor adhesions', 'agglomerate' and 'aggregate'. Mono-grain particles might show an explicit crystal structure, but might also be more or less featureless. Mono-

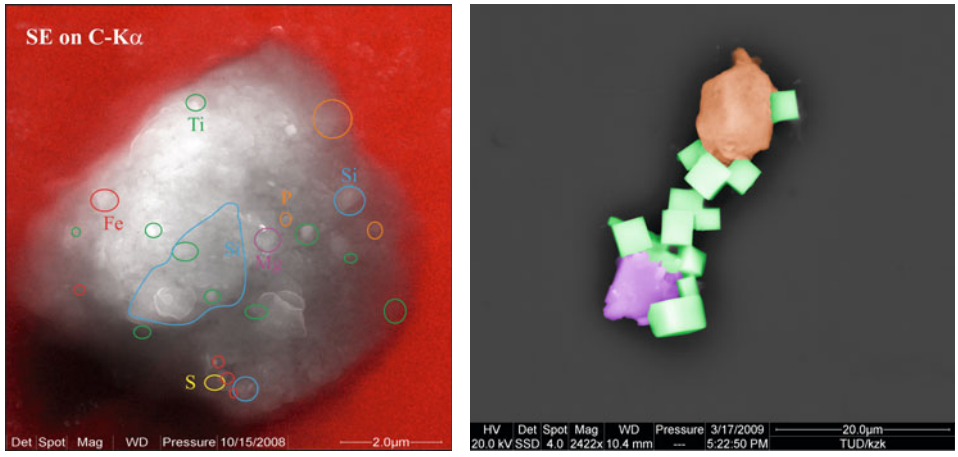

Fig. 1.3. *Left:* clay mineral aggregate (secondary electron image) collected over Morocco in 2006 (for details, see Scheuvens et al. (2011)). The colored spots show regions with enhanced elemental concentrations, indicating the presence of titanium oxides and iron oxi(hydroxi)des, as well as quartz, phosphates, and sulfates. The red background is the carbon fluorescence signal from the substrate and illustrates the thickness of the particle in the lower left corner by 'shadowing' through X-ray shielding from the detector. *Right:* Internal mixture of an alumosilicate (marked in red), sodium chloride (green), and calcium sulfate (violet) collected at Cape Verde (for information on location and sampling, see Kandler et al. (2011a)). In the atmospheric state prior to sampling, the sodium chloride most probably was in solution and recrystallized after sampling; in contrast, the calcium sulfate probably attains its original structure.

grains are not very frequent. The larger, supermicron ones consist usually either of mechanically stable, well-crystallizing minerals like quartz, feldspars, carbonates, and calcium sulfates, or of substances which may have (re-)crystallized in the atmosphere (or even after sampling), like sodium chloride or sulfate. Though the latter compounds might be acquired by atmospheric processing, there is some evidence that they are present in abundance also in desert soils (Osada, 2013). The smaller mono-grains commonly observed are single clay mineral flakes, but may also be metal oxides like rutile or silicates like zircon. More frequently, the type 'main grain with minor adhesions' is found. While the main grains usually consist of the larger, insoluble mono-grains, the adhesions are usually clay flakes which cover the surface of the main grain. Also, a mono-grain particle that acquires a coating through atmospheric processing can be assigned to this category, in which case its abundance is largely dependent on the atmospheric history of the dust sample. The agglomerate and aggregate types are both made of many small grains without a dominating one. Discrimination between them is usually difficult, as the differences are rather gradual in strength of cohesion and compactness: agglomerates are stable in airborne state and might disintegrate on impact or submersion, while aggregates would not. Also, agglomerates can exhibit a higher variability on composition of the single grains, while in aggregates usually one mineral species dominates. Presently, no systematic assessment of the structure-type abundance is available. However, from literature data of single-particle measurements, it seems safe to assume that agglomerates/aggregates dominate over the other types. Figure 1.4 shows examples of the structure types. From quartz (panel a) to K-feldspar with single flakes of clay minerals (b) and large clay mineral grain (c), we can observe a transition from the mono-grain type to the main grain with adhesions; (d) shows a calcite main grain with small clay minerals on top, while (e) and (f) present clay mineral aggregates with rather homogeneous matrix compositions. The particle in (e) is atmospherically aged and contains sodium salts (chloride/nitrate) at the lower and right end. Panels (g) to (i) show the transition from aggregates to agglomerates with more heterogeneous compositions, which are demonstrated by the elemental compositions marked in panel (i).

Mineral dust particles transported in the atmosphere can be processed and become mixed with non-dust material. We can observe this in Fig. 1.4e and i, where sodium compounds – from heterogeneous chemistry and sea-salt mixing – are contained within the particles. The reported abundances of mixed particles range from a few percent (Kandler et al., 2007, 2011a; Matsuki et al., 2010; Zhang et al., 2003) to more than half of the particles (Sullivan et al., 2007a; Zhang et al., 2006; Sullivan and Prather, 2007b). For these partly soluble particles, the structure under higher humidities is unknown; the soluble fraction will accumulate water and form a solution, which then might cover the particle or adhere to it. In the case of agglomerates, the single grains might redistribute and the particles get compacted by surface tension, when the liquid water evaporates under lower humidities.

According to their variety in structures, dust particles can have very different shapes, of which most are irregular or angular. Practically only the mono-grain type can have a symmetric and regular crystal structure, but, as soil material usually suffers physical stress during dust emission (e.g. Shao et al., 2011), most particles show at least damages or irregularities, as can be seen in Fig. 1.4. Clear crystal

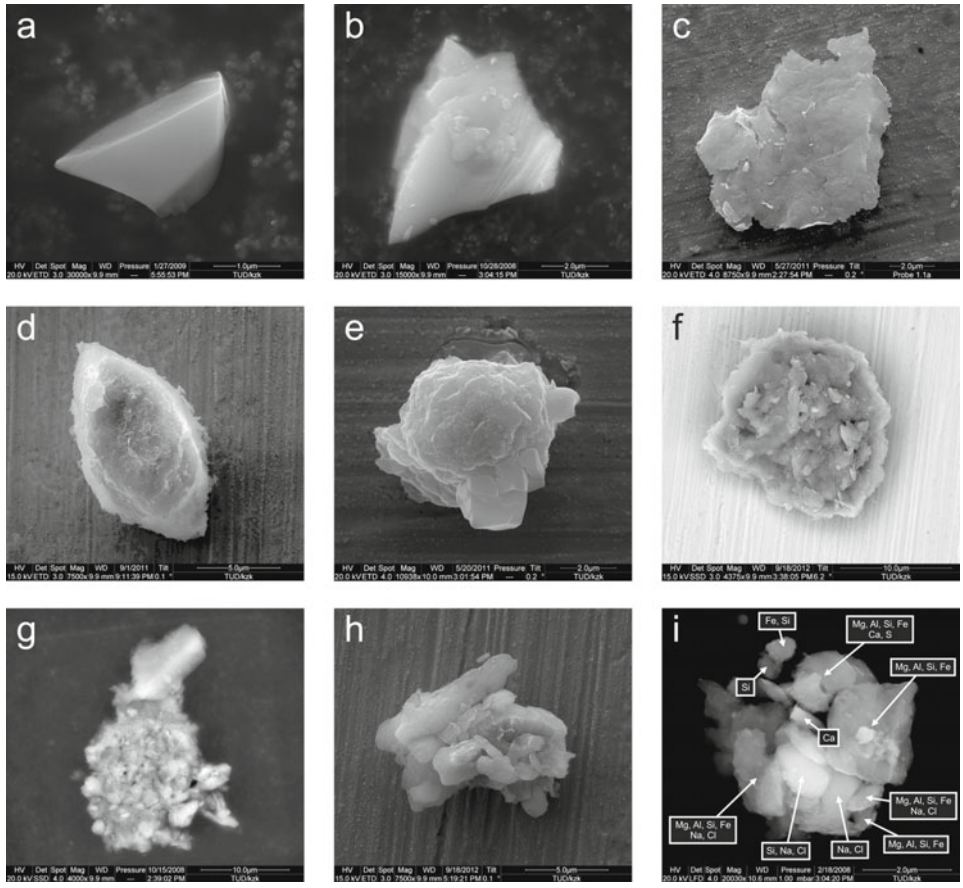

Fig. 1.4. Secondary (panels a-c, e, h) and backscatter (d, f, g, i) electron microscope images of particle structure types found in mineral dust. Panels (a)–(h) were taken from two samples of the same airmass over Morocco (Scheuvens et al., 2011), while (i) was sampled at Praia, Cape Verde from transported Saharan dust (Kandler et al., 2011a). The presence of certain elements marked in image (i) was determined by X-ray fluorescence.

structures can be observed for all mono-grain compounds, but usually not as mono-crystal, instead mostly of a combination of crystals. Particles with a pronounced crystal structure are usually rather smooth, while the main grain particles often possess pronounced surface roughness, in particular in the form of adhering smaller grains, such as clay mineral flakes. A crystal structure in the form of a general particle outline can sometimes still be observed on the main grain type (e.g. Fig. 1.4d). While the mono-grain particles can have smooth, angular surfaces, the main grain particles exhibit roughness due to adhering smaller grains, to the degree that only a preferred orientation of the adhesions according to the underlying surface might remain. The aggregates also have rough surfaces – that is, they possess on their surface irregular oriented regions in the size range of a few to hundreds of nanometers, and no smooth or angular surfaces. In contrast, the agglomerates can possess

larger angular surfaces in irregular orientations (e.g. Fig. 1.4h and i), deriving from their primary grains, but also can have a mixture of these properties. Not much is currently known of the surface roughness of atmospheric dust particles (Formenti et al., 2011). From the few actual surface roughness measurements (Chou et al., 2008) and electron microscopy observations, we might deduce that the size scale of the surface roughness is in the range of hundred(s) of nanometers. However, there is no statistically reliable information available, particularly not on whether the surface roughness depends on the base mineral and whether there are typical grain sizes for certain minerals, which might produce a uniform surface roughness for a particle type.

More information has been collected on the simplified overall particle shape, which is mostly derived by electron-microscopic methods followed by image analysis (e.g. Kandler et al., 2009; Okada et al., 2001; Reid et al., 2003; Coz et al., 2009). A major drawback of this approach is that the image information is usually 2D, while, for optical modeling, 3D shape information is needed. Extrapolation from a 2D to a 3D simplified shape then either requires assumptions on the particles' orientations relative to the image plane or, alternatively, the extrapolation can be used as additional degree of freedom in data inversion (Otto et al., 2009). In particular, the assumptions can introduce a major error in the shape description, as, for example, platelets like clay minerals when oriented flat on a substrate would be described as near spherical. Many simplifying shape descriptors are available (Hentschel and Page, 2003; Rosin, 2003), of which mostly the 2D aspect ratio is chosen, being least dependent on image resolution (Podczeck et al., 1999; Almeida-Prieto et al., 2007). Nevertheless, literature data from different sources are not truly comparable, as there are varying methods in use for aspect ratio calculation, probably biasing the results (Almeida-Prieto et al., 2007). The 2D aspect ratio distribution can be well represented by a modified log-normal distribution (Kandler et al., 2007) with median values in general between 1.5 and 1.7. No significant variation is found between different dust sources; instead, there is a slight dependency on dust composition (Kandler et al., 2007; Coz et al., 2009). Aspect ratios also depend on the particle size (Kandler et al., 2009; Chou et al., 2008; Okada et al., 2001), such that usually the smallest $D < 1$ μm particles have decreasing aspect ratios with decreasing particles size. Also, the large particles $D > 10$ μm have been observed to have lower aspect ratios than those in the 1 μm $< D <$ 10 μm range, where the aspect ratio peaks. This can be explained by particles a few micrometers across consisting of platelets like clay minerals, while towards larger sizes more roundish aggregates or abraded mono-grain particles prevail, with the submicron aerosol particles being predominantly non-dust particles with low aspect ratios. However, we have to keep in mind that the observed 2D values have not shown to be representative for the 3D shape in general. Apart from that, it is safe to say that the highest aspect ratios (needle-like shapes) are formed by mono-grain particles, probably due to their mechanical stability or, in the case of soluble substances, due to their later atmospheric crystallization after the mechanical stress at the emission stage. Three-dimensional simplifying determinations of particle shape are only available in a few cases, mostly as examples (Osada, 2013; Chou et al., 2008). Also, Okada et al. (2001) analyzed several thousand particles of Asian dust with a shadowing technique in the electron microscope to obtain the particle height; they

found a height-to-length ratios between 0.1 and 0.4, implying that the third dimension of the particles is usually smaller than those two readily seen in 2D images, suggesting that indeed the imaged particles tend to be preferentially oriented on the substrate.

A newer approach to measurement of dust particle shape is the application of electron-microscopical stereogrammetry (Lindqvist et al., 2011). With this technique, 3D information of the upper particle half can be obtained in detail, as well as its distance from the grid on the background. These can then be incorporated into a detailed particle model as a basis for calculations of the single-scattering (optical) properties. As of today, only a few particles have been investigated by this approach.

1.2.2 Mineral dust size distribution

Particle size is one of the major parameters determining its optical properties. To assess the radiative properties of an aerosol, the knowledge of its particle size distribution is thus of is of primary importance. For mineral dust, however, the full particle size distribution is challenging to measure, as the particle diameters range from below $D = 100$ nm to larger than 100 μm. Instruments for sizing particles with $D < 10$ μm are readily available (e.g. electrical mobility particle sizers, optical spectrometers, aerodynamic particle sizers); the question at these sizes is rather whether one should – or can – differentiate dust from other particles. In contrast, only a few methods exist to measure size and number concentrations for large airborne particles. This is mainly caused by the 'inlet problem', namely the difficulty of producing an aerosol inlet able to sample representatively particles with diameters considerably larger than $D = 10$ μm. For that reason, size distributions for larger particles are available rather from inlet-free instruments. For example, optical instruments for measuring cloud droplets can be used on board aircraft to measure dust particle size distributions (e.g. Weinzierl et al., 2009), provided that the particle optical properties are well known; otherwise, considerable errors might occur in particular when using forward-scattering instruments (Schumann et al., 2011; Weinzierl et al., 2009). Those instruments usually cannot be used for ground-based measurements, as they need to be moved relatively to the aerosol in a free stream. For ground-based measurements of $D > 30$ μm particles, specialized optical (see an instrument comparison by Mikami et al. (2005)) and acoustical instruments (e.g. Van Pelt et al., 2009)) are available. Furthermore, inlet-free particle collection followed by light-microscopic size analysis can be used for particles with $D > 5$ μm (Kandler et al., 2009). As all of the latter techniques are work-intensive, only small data sets are available for the large particles.

The size distribution of an aerosol is not a conservative property; instead, it is continuously modified by new-particle formation (gas-to-particle and bulk-to-particle conversion as well as heterogeneous chemistry) and removal processes. Subsequently, all available size distribution measurements describe only a certain point in space and time and do not represent a 'general' mineral dust size distribution. Nevertheless, we can observe a systematic behavior in their development. Variability of particle concentrations is highest for the smallest and largest particles (Tanré et al., 2001; Williams et al., 2002); in the case of mineral dust, practically

only the large-particle variability is of interest, because the small-particle variability is mostly due to other aerosol species. For freshly emitted mineral dust, removal is dominated by sedimentation and therefore impacts the largest particles most. Figure 1.5 shows the development of the aerosol size distributions as observed during westward transport out of Africa. First, we observe that the total volume (and mass) concentration is decreasing by about four to five orders of magnitude, governed by the removal of particles from about 200 μm down to 10 μm in diameter. As a result, the volume/mass median diameter shifts from the 100 μm range to the 1 μm range. Second, the variability in the source region can be more than one order of magnitude in concentration, depending on the meteorological and soil conditions. Third, owing to this source variation, concentrations at 1000 km distance can be as high as close to the sources for particles with $D < 20$ μm (see also Kandler et al. (2011b)). When $D > 10$ μm particles have been almost completely removed, the variation decreases. For example, Maring et al. (2003) report that the concentrations of particles smaller than $D = 7$ μm do not change significantly during trans-atlantic transport. Similarly, Reid et al. (2008) observed only minor variability for particles smaller than $D = 10$ μm despite the different emission and transport conditions in the Arabian Gulf region. We may sub-summarize that the form of the size distribution varies considerably near the source area and should always be determined case by case, but further away a priori assumptions might be sufficiently accurate.

Another connected question is how much of the aerosol as a function of particle size actually consists of soil-derived material. This can be addressed by several techniques; distinction between dust and non-dust can be made by hygroscopicity, volatility, optical or chemical properties, assuming that dust is non-hygroscopic and non-volatile, shows a hematite absorption pattern or consists of typical soil minerals, respectively. By all of these techniques, it has been shown for a representative African dust situation that particles with $D > 500$ nm on average consist predominantly of soil material, whereas smaller ones are dominated by non-dust components (Kandler et al., 2009; Weinzierl et al., 2009; Kaaden et al., 2009; Müller et al., 2009). Similar transitional behavior has been reported for Asian dust (Sullivan et al., 2007a). However, this relationship should not be treated as constant: the relative dust abundance between $D = 200$ nm and 3 μm can be quite variable (Kandler et al., 2009, 2011a; Lieke et al., 2011; Schladitz et al., 2011). Not much data are available on the size-resolved dust/non-dust relationship, most likely because the determination is laborious.

Recently, a compilation of measured size distributions of desert-dominated aerosol has become available (Formenti et al., 2011). Assuming that a size distribution is a composite of several lognormally distributed modes – with dust predominant amongst the largest and a minor constituent amongst the smallest particles – allows extracting the 'dust modes' from the available measurements. This assumption seems reasonable in general. However, the observed internal mixing between the components is neglected by this approach. For desert dust close to the source, but neglecting particles with $D > 10$ μm (i.e. an estimate of the long-range transport fraction), these dust modes now have characteristic count median diameters between $D = 1$ and 2 μm and around $D = 5$ and 9 μm (Formenti et al., 2011). Further downwind from the sources, the coarser mode can only be detected

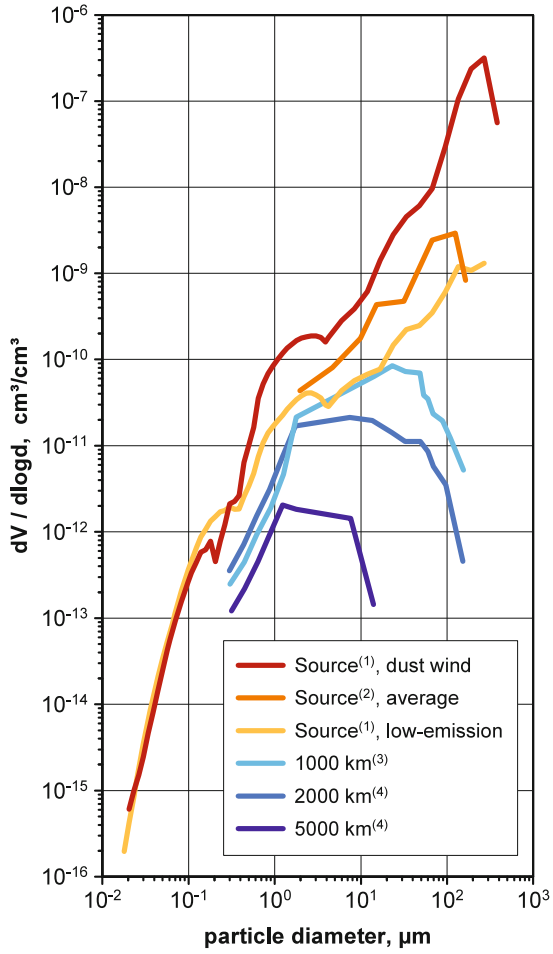

Fig. 1.5. Development of aerosol volume size distributions for Saharan dust with transport distance. (1) Morocco (Kandler et al., 2009); (2) Libya (Schütz and Jaenicke, 1974; Schütz et al., 1981); (3) Cape Verde (Schütz et al., 1981; Jaenicke and Schütz, 1978); (4) Meteor cruises (Schütz et al., 1981).

in a few cases; instead, more frequently, only one dust mode is found with count median diameters of 300 nm to 2 μm.

The mean and the variability of the measured size distributions over northwest Africa (near the source) and Cape Verde (long-range transport) are shown in Fig. 1.6. Note that size distributions for total aerosol are shown, so the small-particle modes are not necessarily representative of dust. It is obvious from the figure that, overall, the variability of the size distributions is fairly low. Further, it can be seen that the variability is higher for transported dust than over the source region. This shows that, on one hand, the dust concentration (strength of the dust modes) is rather a matter of mixing with dust-free airmasses or maybe regional wet removal, and thus exhibits a higher variability in a downwind region not continu-

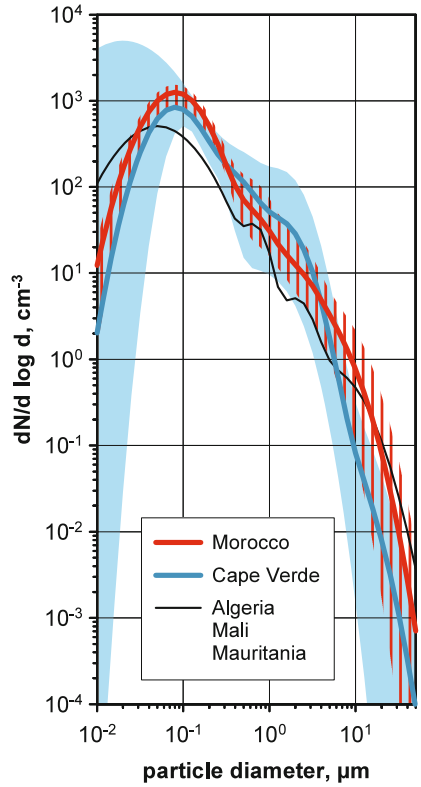

Fig. 1.6. The mean (solid lines) and 3% to 97% variation ranges (shading) of the size distributions determined over Morocco and over Cape Verde (Weinzierl et al., 2011) as well as over Algeria, Mali, and Mauritania (Ryder et al., 2013). For the Cape Verde region, only measurements without considerable biomass-burning influence were taken into account.

ously influenced by dust outbreaks. On the other hand, the faster removal of larger particles by sedimentation predominantly controls the median size of a mode, decreasing this size with increasing transport distance. In contrast, over Morocco, the size distributions have a lower variation, as turbulence tends to mix the single dust outbreaks into a dust reservoir over the continent (Schütz, 1980; Engelstaedter et al., 2006). Nevertheless, also here we still observe a variation in the concentration of more than a factor of five up to more than an order of magnitude at $D = 10\ \mu$m.

1.3 Light-scattering measurements

Dust particles are irregularly shaped and inhomogeneous, and composed of minerals which are typically anisotropic. No analytical, exact solution exists to solve the single-scattering properties of such particles. The solution that comes closest is probably that by Petrov et al. (2011), which applies to any shape that can be described with Laplace series expansion in spherical coordinates, but is limited

to homogeneous targets composed of isotropic material. For other cases for which exact, analytical solutions have been derived, see, for example, Mishchenko et al. (2000). Further, even with exact analytical solutions, there may be practical obstacles for the usage, such as numerical instability of the implementation.

To model dust particles' single-scattering properties, we must therefore choose one of the following three approaches:

- Simplify the problem. Replace dust particles by targets conforming to one of those special geometries for which exact solutions can be obtained.
- Simplify the solver. Use an approximate method which does not solve the problem rigorously, but allows treating the target particle properties accurately.
- Apply brute force. Solve the underlying equations directly using numerical techniques. These can be applied to nearly arbitrary single-scattering problems, but limitations in computer memory and computing power set practical limitations for cases where accurate solutions can be obtained. In general, particles much larger than the wavelength are beyond these methods.

Especially for the first two options, but also for the third option if the accuracy criteria are relaxed or the target particle characteristics are not sufficiently well known, the obtained solutions should be validated. Single-scattering properties measured in a laboratory can provide the reference data needed for this.

The laboratory facilities and the measurement data available for this have been recently reviewed by Muñoz and Hovenier (2011), and we will not go into details here. Rather, we will provide only a short introduction to some such resources. We will not consider field measurements from remote sensing instruments such as lidars or radiometers, because the target particles of these measurements are usually not well characterized (if at all). In addition, often these data are obtained through mathematical inversion of the single-scattering process, where forward single-scattering modeling is required as part of the inversion. Such data would be ill suited for validating (forward) single-scattering methods. The laboratory data we consider present measured single-scattering properties that have been obtained without any modeling or analytical single-scattering computations. Unfortunately, this does not mean that these data could always be applied for validation purposes without some modeling.

Of particular relevance for validation are measurements of the full scattering matrix (see section 1.4.1, Eq. (1.1)), because it fully describes the single-scattering event, except for absorption. The scattering matrix contains up to seven independent elements, which are all functions of the physical properties of the scatterers and the scattering geometry. With the measured scattering matrix, both the intensity and polarization characteristics (including depolarization) of the scattered radiation, predicted by the chosen modeling approach, can be validated. For various types of dust particles, full scattering matrices measured in the laboratory are available at the Amsterdam-Granada light-scattering database (Muñoz et al., 2012). The database also contains the measured size distribution for all the samples, as well as an estimate for the refractive index, which are needed when trying to reproduce the measured scattering matrix by modeling.

When comparing simulated and measured scattering matrices, one must realize that the measured matrices are often in arbitrary units, so they differ from the

simulated matrices by an unknown normalization coefficient. To renormalize the measured matrices, the normalization integral (section 1.4.1, Eq. (1.3)) can be applied. This requires, however, that the measurements cover the whole angular range to be integrated, which usually is not the case. If the size distribution of the sample is known and the refractive index can be estimated reasonably well, it may be possible to fill the gaps in the measurements by modeled values. This is thus one of those instances where validation based on measurements requires some light-scattering simulations before the measured data can be applied for the purpose. The impact of possibly erroneous renormalization on the validation must then be kept in mind. In particular for dust, probably all size distribution measurements are subject to uncertainties. For different renormalization procedures suggested, see, for example, Liu et al. (2003) and Kahnert and Nousiainen (2006, 2007).

The measurement of the whole scattering matrix is quite demanding (Muñoz et al., 2010), requiring multiple measurements with varying polarization states for the incident radiation. It is much simpler to measure only part of the scattering matrix, and the resulting data can be supplemented with other independent data to still provide a reasonable base for validation. For example, simultaneous infrared extinction spectrum measurements have been used (Meland et al., 2012; Alexander et al., 2013). The requirement of simultaneously reproducing scattering and extinction data provides a much more stringent test for the model than either set of data could, alone.

1.4 Light-scattering modeling

A wide variety of modeling approaches have been used for the purpose of estimating, via numerical computations, how natural dust particles interact with electromagnetic radiation. The purpose of this section is to review these approaches. The first subsection (1.4.1) introduces the basic concepts that are used to characterize how dust particles, either individually or as an ensemble, scatter and absorb light. The next two subsections (1.4.2 for simple and 1.4.3 for complex model particles) address different modeling approaches and how they perform in mimicking scattering by real dust particles. Section 1.4.4 focuses on how certain physical characteristics of the dust particles, in particular the surface roughness, internal inhomogeneity, or material anisotropy of the component minerals of the dust particles, influence their single-scattering properties.

1.4.1 Definitions

The interaction of electromagnetic radiation with particles is described by the single-scattering properties. Often, in the literature, these are also called optical properties, although this is a less preferable term due to its non-consistent use in different fields.

Single-scattering events are commonly described by scattering matrices that relate the properties of the incident and scattered radiation. Here we adapt the Mueller matrix formalism which relates the incident and scattered radiation expressed as Stokes vectors $[I, Q, U, V]^T$, resulting in a 4×4 scattering matrix. The